Functionalization of Graphene *via* 1,3-Dipolar Cycloaddition

Mildred Quintana,[†] Konstantinos Spyrou,[‡] Marek Grzelczak,[†] Wesley R. Browne,[§] Petra Rudolf,[‡] and Maurizio Prato[†,*]

[†]Center of Excellence for Nanostructured Materials (CENMAT) and INSTM, Unit of Trieste, Dipartimento di Scienze Farmaceutiche, University of Trieste, Piazzale Europa 1, I-34127 Trieste, Italy, [‡]Zernike Institute for Advanced Materials, and [§]Stratingh Institute for Chemistry, University of Groningen, Nijenborgh 4, NL-9747AG Groningen, The Netherlands

ABSTRACT Few-layer graphenes (FLG) produced by dispersion and exfoliation of graphite in *N*-methylpyrrolidone were successfully functionalized using the 1,3-dipolar cycloaddition of azomethine ylides. The amino functional groups attached to graphene sheets were quantified by the Kaiser test. These amino groups selectively bind to gold nanorods, which were introduced as contrast markers for the identification of the graphene reactive sites. The interaction between gold nanorods and functionalized graphene was followed by UV—vis spectroscopy. The presence of the organic groups was confirmed by X-ray photoelectron spectroscopy and thermogravimetric analysis. The sheets were characterized by transmission electron microscopy, demonstrating the presence of gold nanorods distributed uniformly all over the graphene surface. This observation indicates that reaction has taken place not just at the edges but also at the internal C═C bonds of graphene. Our results identify exfoliated graphene as a considerably more reactive structure than graphite and hence open the possibility to control the functionalization for use as a scaffold in the construction of organized composite nanomaterials.

KEYWORDS: graphene · carbon nanostructures · 1,3-dipolar cycloaddition · gold nanorods · nanoscaffold

Graphene is a single layer of carbon atoms arranged in a hexagonal lattice and one of the few structures that are stable in two dimensions.[1] Its extraordinary properties, such as high carrier mobility, half-integer quantum Hall effect at room temperature,[2] spin transport,[3] high elasticity,[4] electromechanical modulation, and ferromagnetism,[5] have made graphene a very promising candidate as a robust atomic-scale scaffold in the design of new nanomaterials.[6] The integration of graphene sheets with metal or semiconductor nanoparticles for the creation of new biosensors,[7] energy storage materials,[8] and fuel cells[9] has been proposed. Modification of the carbon network by grafting atoms or molecules is important in the design of graphene-based nanoelectronics because this provides a means to dope the material.[10] For the development of optoelectronic devices, functionalization of graphene with photoactive molecules can provide interesting donor—acceptor nanohybrids.[11]

Before one can chemically manipulate graphene and transform it into various functional structures or integrate it with other materials to form nanodevices, two preliminary steps are necessary: first, graphite has to be chemically exfoliated into individual or few-layer sheets, and second, the graphene sheets have to be stabilized. Recently, high-yield liquid-phase exfoliation of graphite into individual sheets by stabilization through interactions with the solvent was reported.[12] This methodology opens the way to carry out different organic reactions on graphene in order to produce specific structures for functional devices.

An interesting reaction to test on graphene is the 1,3-dipolar cycloaddition of azomethine ylides because this reaction has been extensively used for the chemical modification of carbon nanotubes[13] (CNTs) and fullerenes[14] with applications in different fields such as solar energy conversion and biosensors.[15] CNTs and fullerenes differ from graphene in that they present a curvature which mixes some sp^3 character into the sp^2 hydridization. In fullerenes and CNTs, the curvature has been put in relation with the reactivity of the carbon nanostructure: the stronger the curvature, the higher the reactivity.[16] In graphene instead, the sheet edges are considered the most reactive sites.[17]

With this contribution, we demonstrate that even if the reactivity of graphene differs from that of fullerenes and CNTs, the 1,3-dipolar cycloaddition can be performed efficiently and yields a highly functionalized material.[18] To prove this, we identified the reactive sites on graphene layers by introducing amino groups quantified by the Kaiser test. These free amino groups selectively bind to gold nanorods (AuNRs), which were employed as contrast markers.

*Address correspondence to prato@units.it.

Received for review April 26, 2010 and accepted May 16, 2010.

Published online May 26, 2010.
10.1021/nn100883p

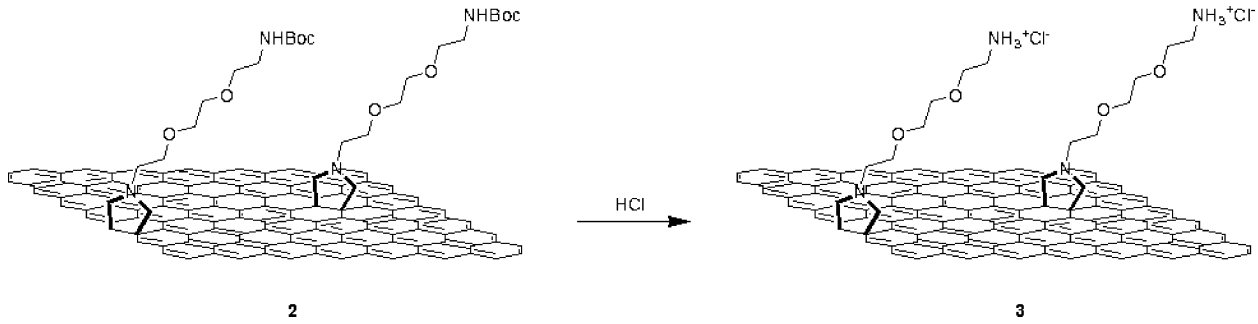

2 3

Scheme 1. Representation of functionalized graphene derivatives before and after the cleavage of the Boc protecting groups.

The interaction between AuNRs and functionalized graphene was followed by UV−vis spectroscopy, while the morphological changes were characterized by transmission electron microscopy (TEM). The presence of the organic groups and their interaction with AuNRs were verified by X-ray photoelectron spectroscopy (XPS). Thermogravimetric analysis (TGA) confirmed the functionalization degree of the products. In short, here we prove that 1,3-dipolar cycloaddition of azomethine ylides on graphene produces a highly functionalized material that provides a platform for the construction of a nanocomposite material using AuNRs.

RESULTS AND DISCUSSION

To obtain graphene sheets **1**, we have used the solvent extraction procedure[12] because by this technique it is possible to effectively produce single and few graphene layers without the use of intercalants,[19] polymers,[20] or surfactants,[21] which might interfere with the organic reaction. Functionalized graphene **2** was prepared by condensation of paraformaldehyde with a modified α-amino acid ($BocNHCH_2CH_2OCH_2CH_2OCH_2CH_2NHCH_2COOH$), followed by the deprotection of the *t*-butyl carbamate group (Boc group) to afford **3** (Scheme 1).

To verify the presence of free amino groups in the products, we have performed the quantitative Kaiser test.[22] For graphenes **1** and **2**, we obtained a negative test value, while following the cleavage of the Boc group, the amount of amine functions in **3** was calculated in the range of 640 ± 70 μmol/g of material. This is a high value if one takes into account only the functionalization of the edges of graphene sheets considered as the most reactive sites. This is the first indication that 1,3-dipolar cycloaddition must take place also in the central carbon−carbon bonds of graphene layers.

The presence of organic groups on the graphene sheets was further analyzed by TGA. TGA plots under N_2 of graphite and products **1** and **2** are shown in Figure 1. The overall weight loss of exfoliated graphite, product **1**, is ~1.5%, which can be attributed mostly to the solvent molecules stabilizing graphene sheets.[12] The observed weight loss for product **2** is 15%. The degree of functionalization is estimated to be approximately 1 functional group in 128 carbon atoms and is in good agreement with the Kaiser test amine content.

To visualize the functional groups on the graphene sheets, we have used gold NRs which not only can be attached to free amino group[23] but also possess interesting optical properties arising from localized surface-plasmon resonances.[24] In fact, due to the shape anisotropy of NRs, two well-defined types of resonances occur, parallel and transversal to the long axis of the rod. The sensitivity of the longitudinal plasmon band to interparticle interaction gives rise to strong changes in the absorption spectra, which are directly related to a plasmon coupling effect.[25] Taking advantage of this behavior, we have used AuNRs as contrast marker agents sensitive to aggregation. To this purpose, prior to the graphene conjugation experiment, CTAB was exchanged with poly(vinylpyrrolidone) (PVP) as previously reported[26] to allow for transfer into DMF without aggregation. The AuNR solution was then mixed with **1**, **2**, or **3** in DMF and monitored by UV−vis−NIR spectroscopy for 6 h, as shown in Figure 2. The maximum of the longitudinal plasmon band (LPB) of initial, well-dispersed AuNRs is marked with a dashed line. The LPB of AuNRs mixed with **1** and **2** remains unchanged, indicating no further interaction with either as-exfoliated or NH-Boc-functionalized graphene sheets. Conversely, in the case of rods mixed with **3**, the LPB was broadened and red-shifted by about 110 nm, a behavior that indicates aggregation on the flat surface.[27]

TEM analysis confirmed that AuNRs are indeed grafted onto the graphene sheets. Figure 3 shows the

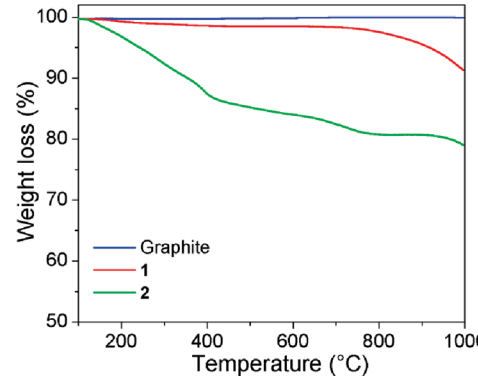

Figure 1. Thermograms of graphite, along with products 1 and 2.

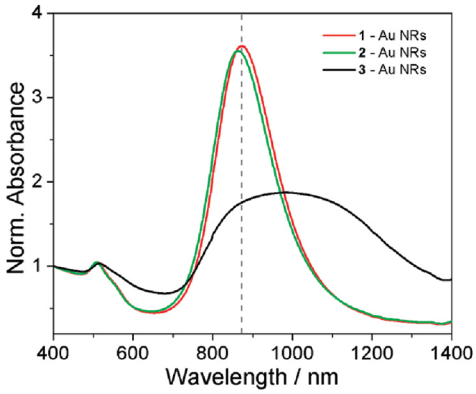

Figure 2. UV−vis−NIR absorption spectra of AuNRs mixed with 1 (black), 2 (red), and 3 (blue), showing aggregation of nanorods on amine-functionalized graphene sheets. The dashed line at 871 nm corresponds to the position of the longitudinal plasmon band of isolated gold nanorods in DMF (Supporting Information). All spectra are normalized at 400 nm for better comparison.

TEM images of all products; a difference observed in the morphology of products **1** (Figure 3a) and **2** (Figure 3b) is a decrease in the average size of functionalized products, which was found to be 2.69 ± 1.39 μm (31 images). The reduction in the average size after the reaction is possibly a consequence of the higher reactivity of graphene borders. Most importantly, the distribution of AuNRs all over the graphene surfaces was seen only for **3** (Figure 3c). In order to confirm the specific affinity of AuNRs to product **3**, control experiments were performed in which products **1** and **2** were mixed with nanoparticles, showing no interaction (Figure S3a,b in Supporting Information), which is consistent with the observations from UV−vis−NIR experiments (Figure 2). Uniform distribution of the nanoparticles on the functionalized FLG indicates that the reaction has taken place not just at the edges of the graphene sheets but also at the central C═C. This is a very interesting result since it identifies exfoliated graphene as a considerably more reactive structure than graphite and hence opens the possibility to control the degree of graphene functionalization to obtain specific nanostructures.

Figure 4 shows the Raman spectra of the graphene products compared to graphite. In the graphite spectra, there are two intense features, which are the vibrational G band and the two-phonon 2D band. The second-order Raman 2D band is sensitive to the number of layers in graphene, as has been proposed in the literature.[28] Unfortunately, in our Raman spectra, we are not able to identify single-layer graphenes, which have a very sharp and symmetric band. Nevertheless, by the position and the shape of the 2D band at about 2700 cm^{-1} and the relative intensity of the G and 2D bands, we observe most of the aggregates as few-layer graphenes (FLG), as reported in Figure 4. A clear difference between functionalized and nonfunctionalized FLG is the appearance of the disorder D band at about 1350 cm^{-1}. In **1**, the D band is weak and may arise from

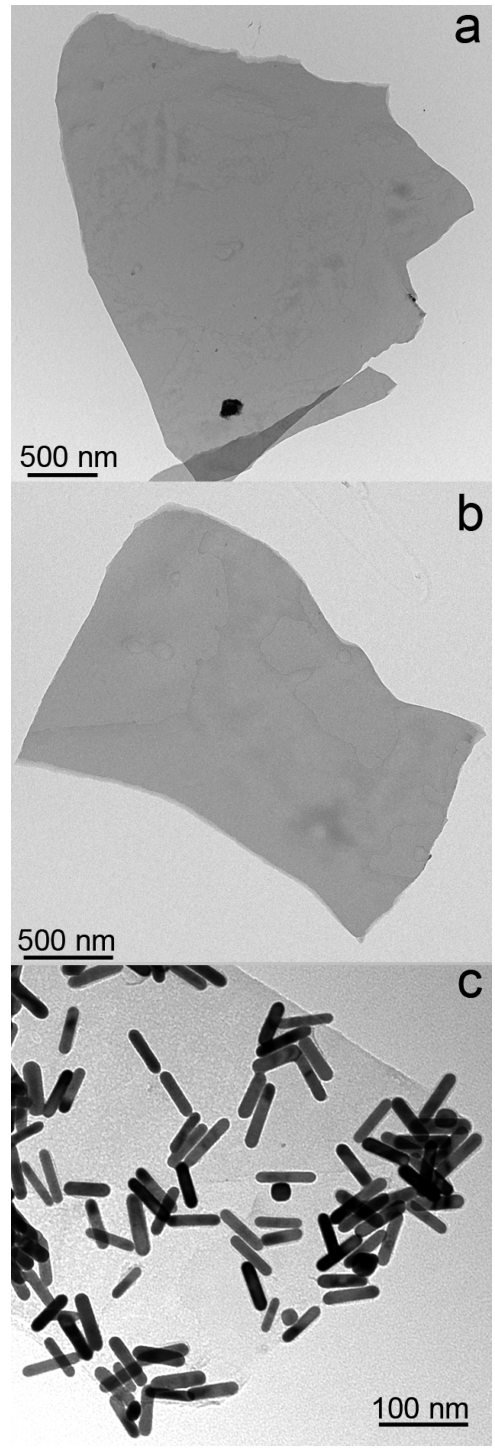

Figure 3. TEM images of (a) 1 stabilized graphene in NMP, (b) 2 functionalized Boc-protected graphene, (c) 3 functionalized graphene after the cleavage of the Boc group and mixed with AuNRs.

the presence of defects at the graphene edges and the interaction with the substrate. An important feature of the D band is that its intensity decreases with the increase of graphene thickness and is invisible for bulk graphite, demonstrating that defects are more easily introduced into thinner graphene sheets,[29] allowing the organic functionalization preferentially on monolay-

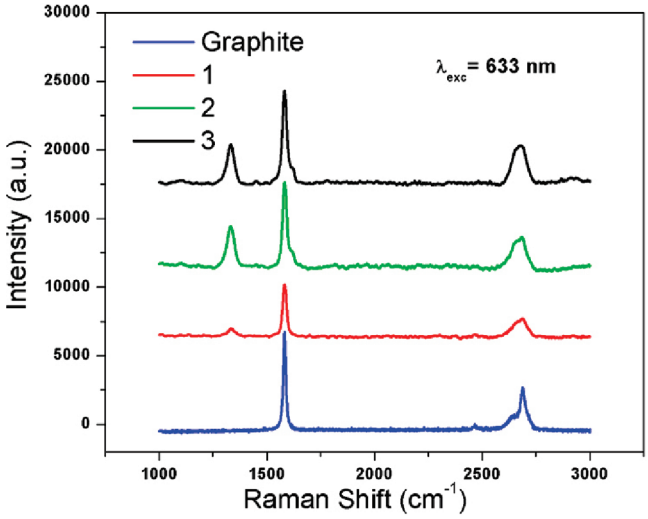

Figure 4. Raman spectra of raw graphite and few-layer graphenes before and after functionalization.

ers and FLG. As observed, for products **2** and **3**, there is an increase in the intensity of the D band associated with the presence of defects on the lattice as a result of the organic functionalization. As a consequence, after 1,3-dipolar cycloaddition, it is possible to increase the concentration of graphene layers obtaining stable dispersions of 0.1 mg/mL, as calculated by UV−vis spectroscopy.

To confirm the presence of the organic groups involved in the reaction, all products were characterized by X-ray photoelectron spectroscopy, a direct method for determining the surface elemental composition of a material. The C1s core level photoemission spectra of **2** and of the graphite used as starting material are shown in Figure 5a,b, respectively. The spectral analysis procedure consists of mathematically reconstructing the spectrum with a minimum number of peaks consistent with the raw data and the molecular structure, with the simplification of assuming equivalent carbon atoms depending on their environment. On this basis, four contributions to the carbon 1s core level region recorded for the functionalized graphene can be

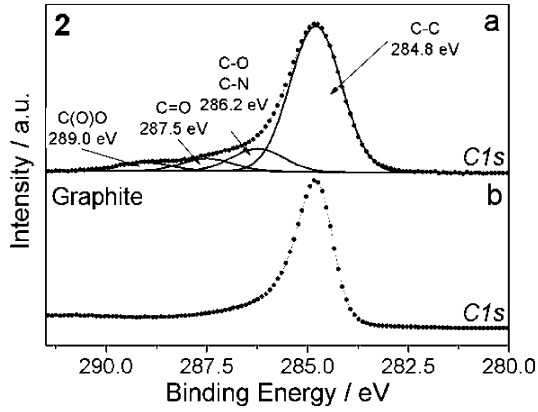

Figure 5. Photoemission spectra and fit of the C1s core level region and fit of (a) product 2 and (b) graphite dispersed on Au/mica.

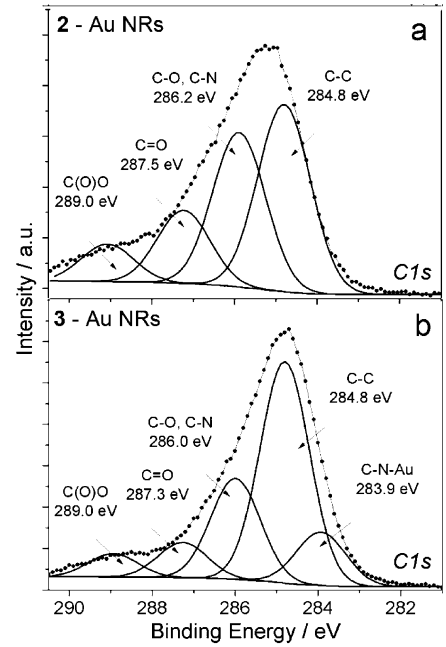

Figure 6. Photoemission spectra and fit of the C1s core level region of (a) 2-AuNRs (b) 3-AuNRs, dispersed on Al.

identified: A first main peak at a binding energy of 284.8 eV is assigned to the C−C bonds of the graphene sheet. A second peak due to carbons bound to oxygen and to nitrogen is seen at 286.2 eV, while the C═O and O−C═O contributions are found at 287.5 and 289.0 eV, respectively. The presence of these carbon atoms clearly confirms the successful functionalization of graphene. The graphite C1s spectrum (Figure 5b) plotted for comparison verifies the good quality of the sample. Figure 6 shows the photoemission spectra and fit of the C1s core level region of two types of functionalized graphene after exposure to Au nanorods: (a) **2**-Au and (b) **3**-Au. Comparison with the C1s peak of functionalized graphene discussed above (Figure 6a) demonstrates that only the spectrum of product **3**-Au (Figure 6b) shows an additional peak at 283.9 eV binding energy, attributed to the C−N−Au bond.[30,31] This means that the amino groups recognize the AuNRs, as previously shown by UV−vis−NIR spectroscopy. The other difference between the spectra in Figure 6 is that, of course, the carbonyl peak is more intense for **2** (Figure 6a).

Additional evidence for the presence of the Boc groups comes from the O1s core level photoemission spectra for **2** and **3** shown in Figure 7. In fact, as expected, the contributions from carbonyl and carboxyl groups are more important for product **2** (Figure 7a). From the fit of the O1s and the C1s spectra, we can deduce the intensities of the different contributions and find that the carbonyl and carboxyl group intensities in the O1s spectra totally agree with the corresponding C1s intensities. From these intensities, we can calculate the atomic percentages of the elements present after application of the two functionalization procedures.

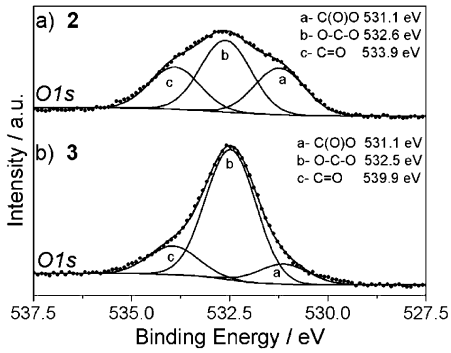

Figure 7. Photoemission spectra and fit of the O1s core level region of (a) 2 and (b) 3 dispersed on Au/mica.

This quantitative analysis is reported in Table 1 and shows a decrease of the oxygen levels from ~15 atomic % in product **2** to ~4 atomic % in product **3**.

Figure 8 shows the N1s core level photoemission spectra of products **2** and **3**. In Figure 8a, the N-Boc nitrogen is identified at 400.4 eV, in analogy to a similar fullerene derivative,[32] while the pyrrolidine nitrogen is located at 398.9 eV. Therefore, from the fit of the spectra for **3** (Figure 8b), we can identify the positively charged (NH_3^+) species of the amine group at a binding energy of 401.1 eV as well as the nitrogen of the pyrrolidine at 399.7 eV, whose shift with respect to **2** is probably due to partial protonation. On the basis of the XPS analysis, we can assume that the interactions between Au nanoparticles with **3** are driven by two different interactions, the formation of amine-gold bonding[33] (Figure 6b) and the electrostatic recognition between protonated amine and PVP stabilizer.[34]

TABLE 1. Atomic Composition of Functionalized Graphene[a]

atomic %	product 3	error %	product 2	error %
carbon	95.2	±1.9	82.9	±1.7
oxygen	4.1	±0.3	15.2	±0.9
nitrogen	0.7	±0.1	1.9	±0.2

[a]X-ray photoelectron spectroscopy cannot reveal hydrogen; the atomic percentage of hydrogen is therefore set to zero.

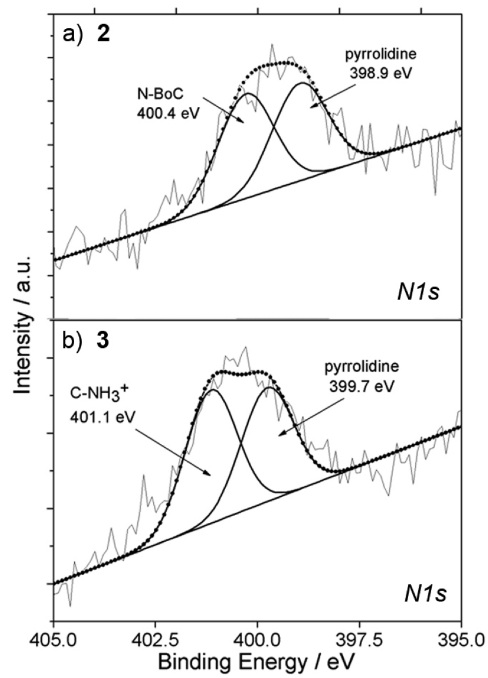

Figure 8. Photoemission spectra and fit of the N1s core level of (a) 2 and (b) 3 dispersed on Au/mica.

CONCLUSION

In summary, we have successfully produced functionalized graphene layers by condensation of a protected α-amino acid and paraformaldehyde followed by the deprotection of the Boc group. This derivative can be easily integrated with AuNRs that serve as contrast markers for the identification of the reactive sites and produces a nanocomposite material that can be used for diverse applications.

Further chemical modifications of graphene-functionalized **3** can be easily envisioned, such as introduction of photoexcitable donor−acceptor groups for photoinduced charge-transfer studies in photovoltaic devices.

EXPERIMENTAL SECTION

Chemicals. Tetrachloroauric acid ($HAuCl_4 \cdot 3H_2O$), silver nitrate ($AgNO_3$), sodium borohydride ($NaBH_4$), ascorbic acid, concentrated HCl, cetyltrimethylammonium bromide (CTAB), and poly(vinylpyrrolidone) (PVP, M_w = 40 000) were purchased from Aldrich. All solvents were obtained from commercial suppliers and used without further purification. (2-[2-(2-*tert*-Butoxycarbonylaminoethoxy)ethoxy]ethylamino) acetic acid was synthesized according to reported procedure.[35] Milli-Q water with a resistivity of 18.2 MΩ · cm was used in gold nanorod synthesis. Graphite was purchased from Bay Carbon, Inc. (SP-1 graphite powder, www.baycarbon.com).

Characterization Techniques. The optical characterization was carried out by UV−vis−NIR spectroscopy with a Cary 5000 spectrophotometer using 10 mm path length quartz cuvettes. TEM measurements were performed on a TEM Philips EM208, using an accelerating voltage of 100 kV. Samples were prepared by drop casting from the dispersion onto a TEM grid (200 mesh, nickel, carbon only). TGA, of approximately 1 mg of each compound, was recorded on a TGA Q500 (TA Instruments) under N_2, by equilibrating at 100 °C, and following a ramp of 10 °C/min up to 1000 °C. X-ray photoelectron spectroscopy (XPS) data were collected using an SSX-100 (Surface Science Instruments) spectrometer equipped with a monochromatic Al Kα X-ray source ($h\nu$ = 1486.6 eV); the photoelectron take off angle was 37°, and the energy resolution was set to 1.5 eV. An electron flood gun was used to compensate for sample charging; the base pressure during the measurement was 3×10^{10} mbar. Binding energies were referenced to the Au $4f_{7/2}$ [1] and the Al 2p [1] core levels of the substrates on which the graphitic material was deposited. Spectral analysis included a Shirley background subtraction and peak separation using mixed Gaussian−Lorentzian functions in a least-squares curve-fitting program (Winspec) developed in the LISE laboratory of the Facultés Universitaires Notre-Dame de la Paix, Namur, Belgium. For N1s line, we employed a linear background subtraction due to low peak intensity, which does not al-

low for Shirley background subtraction. The photoemission peak areas of each element used to estimate the amount of each species on the surface were normalized by the sensitivity factors of each element tabulated for the spectrometer used. The substrates were evaporated gold films supported on mica (cleaned in an ozone discharge for 15 min, followed by sonication in ethanol for 20 min immediately before being employed) or Al foil (purity 99.99%, Goodfellow, UK), which was polished (Brasso metal polish, Reckitt Benckiser UK Ltd., UK) to remove most of the impurities from the surface, sonicated in ethanol for 20 min, and dried in an oven (Thermo Electron Corporation, USA) at 65 °C immediately before being employed. The samples were dispersed in NMP, then a drop was cast on the substrate and dried under vacuum. Raman spectra were recorded with an Invia Renishaw microspectrometer (50×) equipped with He−Ne laser at 633 and Ar laser at 488 nm. Samples were recorded from drops of the dispersions of graphene products in NMP deposited on glass surfaces. Surfaces were left to dry under vacuum.

Graphite Exfoliation, Product 1. Twenty-four milligrams of graphite was dispersed in 200 mL of NMP and sonicated for 30 min in a low power sonic bath (2510 Branson). The resultant dispersion was then centrifuged using a Hettich Universal 320 centrifuge for 90 min at 500 rpm. Thereafter, decantation was carried out by pipetting off the top half of the dispersion.

1,3-Dipolar Cycloaddition on Graphene, Product 2. Fifty mL of exfoliated graphite solution was used to carry out the reaction. The graphene concentration of the solution was calculated by the optical characterization reported by Coleman and co-workers.[12] The concentration was normally found to range from 0.01 ± 0.005 mg/mL. To perform the organic reaction, 1.5 equiv with respect to graphene of modified amino acid[35] and paraformaldehyde was added to the graphene suspension. The reaction mixture was heated at 125 °C under magnetic stirring, while the reagents were added each 24 h for 5 days. The resulting mixture was filtered with a Millipore system (JH 0.45 μm filter), and the solid was washed thoroughly with methanol until the solvent was clear. The product was dispersed in 20 mL of DMF by mild sonication.

Deprotection of the Boc Group, Product 3. To cleave the Boc group from functionalized graphene, product **2** was dispersed by sonication in a 4 M solution of HCl in dioxane. The solution was stirred magnetically for 5 h and then was filtered and washed thoroughly first with DMF and finally with methanol. After drying the solvent, the solid was dispersed in 20 mL of DMF, and the final concentration of FLG was measured by UV−vis spectroscopy and found to range between 0.025 ± 0.005 mg/mL.

Kaiser Test. The amount of free amino groups per gram of graphene was measured in 0.5 mL solutions of products **1**, **2**, and **3** in DMF by the quantitative Kaiser test (Sigma-Aldrich). DMF was used as a blank sample. The Kaiser test is a colorimetric assay that reveals quantitatively the presence of primary amino groups and, therefore, the number of functional groups attached to graphene after reaction.

Gold Nanorod Preparation, AuNRs. A solution of gold seed was prepared by borohydride (30 mM, 0.3 mL) reduction of $HAuCl_4$ (0.25 mM, 5 mL) in aqueous cetyltrimethylammonium bromide (CTAB) solution (0.1 M). An aliquot of the seed solution (24 μL) was added to a growth solution (10 mL) containing CTAB (0.1 M), $HAuCl_4$ (0.5 mM), ascorbic acid (0.8 mM), silver nitrate (0.12 mM), and HCl (18.6 mM). The mixture was left undisturbed for 4 h at 27 °C.

Surface Functionalization of Gold Nanorods—PVP Coating. Typically, a suspension of as-prepared gold nanorods (10 mL) was centrifuged at 8000 rpm for 15 min, and the precipitate was redispersed in Milli-Q water (5 mL). Subsequently, 5 mL of CTAB-coated gold nanorods was mixed with an aqueous solution of PVP (1.2 mM, 5 mL) and stirred overnight. The mixture was centrifuged at 4500 rpm for 60 min, and the precipitate was redispersed in 5 mL of DMF under sonication.

Graphene−AuNR Composites. One milliliter of solutions of products **1**, **2**, and **3** was separately mixed with 2 mL of AuNR solution each. After 6 h of incubation, the graphene−AuNR composite solution was washed by centrifugation (1500 rpm, 20 min) and redispersed in DMF.

Acknowledgment. This work was financially supported by the University of Trieste, INSTM, Italian Ministry of Education MIUR (Cofin Prot. 20085M27SS and Firb RBIN04HC3S), the Dutch Foundation for Fundamental Research on Matter (FOM), the Breedtestrategie program of the University of Groningen, and the MSC+ program of the Zernike Institute for Advanced Materials. We are extremely grateful to Prof. Moreno Meneghetti (University of Padova) for great help with Raman spectroscopy. We also thank Mr. Claudio Gamboz (University of Trieste) for kind help with TEM experiments.

Note added after ASAP publication: Due to a production error, the graphite solution in Product 2 in the Experimental Section was incorrectly reported as microliters on May 26, 2010. The corrected version was published on June 3, 2010.

Supporting Information Available: Additional experimental information and figures. This material is available free of charge *via* the Internet at http://pubs.acs.org.

REFERENCES AND NOTES

1. (a) Bernard, A. S.; Shook, I. K. Thermal Stability of Graphene Edge Structure and Graphene Nanoflakes. *J. Chem. Phys.* **2008**, *128*, 094707. (b) Meyer, J. C.; Geim, A. K.; Katsnelson, M. I.; Novoselov, K. S.; Booth, T. J.; Roth, S. The Structure of Suspended Graphene. *Nature* **2007**, *446*, 60–63.
2. (a) Novoselov, K. S.; Geim, A. K.; Morozov, S. V.; Jiang, D.; Katsnelson, M. I.; Grigorieva, I. V.; Dubonos, S. V.; Firsov, A. A. Two-Dimensional Gas of Massless Dirac Fermions in Graphene. *Nature* **2005**, *438*, 197–200. (b) Zhang, Y.; Tan, J. W.; Stormer, H.; Kim, L. P. Experimental Observation of the Quantum Hall Effect and Berry's Phase in Graphene. *Nature* **2005**, *438*, 201–204.
3. Tombros, N.; Jozsa, C.; Popinciuc, M.; Jonkman, H. T.; van Wees, B. J. Electronic Spin Transport and Spin Precession in Single Graphene Layers at Room Temperature. *Nature* **2007**, *448*, 571–574.
4. Kim, K. S.; Zhao, Y.; Jang, H.; Lee, S. Y.; Kim, J. M.; Kim, K. S.; Ahn, J.-H.; Kim, P.; Choi, J; Hong, B. H. Large-Scale Pattern Growth of Graphene Films for Stretchable Transparent Electrodes. *Nature* **2009**, *457*, 706–710.
5. Wang, Y.; Huang, Y.; Song, Y.; Zhang, X. Y.; Ma, Y. F.; Liang, J. J.; Chen, Y. S. Room Temperature Ferromagnetism of Graphene. *Nano Lett.* **2009**, *9*, 220–224.
6. Elias, D. C.; Nair, R. R.; Mohiuddin, T. M. G.; Morozov, S.; Blake, V. P.; Halsall, M. P.; Ferrari, A. C.; Boukvalov, D. W.; Katsnelson, M. I.; Geim, A. K.; Novoselov, K. S. Control of Graphene's Properties by Reversible Hydrogenation: Evidence for Graphene. *Science* **2009**, *323*, 610–613.
7. (a) Schedin, F.; Geim, A. K.; Morozov, S. V.; Hill, E. W.; Blake, P.; Katsnelson, M. I.; Novoselov, K, S. Detection of Individual Gas Molecules Adsorbed on Graphene. *Nat. Mater.* **2007**, *6*, 652–655. (b) Lu, J.; Do, I.; Drzal, L. T.; Worden, R. M.; Lee, I. Nanometal Decorated Exfoliated Graphite Nanoplatelet Based Glucose Biosensor with High Sensitivity and Fast Response. *ACS Nano* **2008**, *2*, 1825–1832.
8. Stoller, M. D.; Park, S.; Zhu, Y.; An, J.; Ruoff, R. S. Graphene-Based Ultracapacitors. *Nano Lett.* **2008**, *8*, 3498–3502.
9. Si, Y.; Samulski, E. T. Exfoliated Graphene Separated by Platinium Nanoparticles. *Chem. Mater.* **2008**, *20*, 6792–6797.
10. (a) Westervelt, R. M. Graphene Nanoelectronics. *Science* **2008**, *320*, 324–325. (b) Chen, W.; Chen, S.; Qi, D. C.; Gao, X. Y.; Wee, A. T. S. Surface Transfer p-Type Doping of Epitaxial Graphene. *J. Am. Chem. Soc.* **2007**, *129*, 10418–10422.
11. (a) Williams, G.; Seger, B.; Kamat, P. V. TiO_2−Graphene Nanocomposites. UV-Assisted Photocatalytic Reduction of Graphene Oxide. *ACS Nano* **2008**, *2*, 1487–1491. (b) Xu, Y.; Liu, Z.; Zhang, X.; Wang, Y.; Tian, J.; Huang, Y.; Ma, Y.; Zhang, X. Y.; Chen, Y. A Graphene Hybrid Material Covalently Functionalized with Porphyrin: Covalent and Optical Limiting Property. *Adv. Mater.* **2009**, *21*, 1275–1279.

12. Hernandez, Y.; Nicolosi, V.; Lotya, M.; Blighe, F. M.; Sun, Z.; De, S.; McGovern, I. T.; Holland, B.; Byrne, M.; Gunko, Y. K.; Boland, J. J.; Niraj, P.; Duesberg, G.; Krishnamurthy, S.; Goodhue, R.; Hutchison, J.; Scardaci, V.; Ferrari, A. C.; Coleman, J. N. High Yield Production of Graphene by Liquid-Phase Exfoliation of Graphite. *Nat. Nanotechnol.* **2008**, *3*, 563–568.
13. (a) Georgakilas, V.; Kordatos, K.; Prato, M.; Guildi, D. M.; Holzinger, M.; Hirsch, A. Organic Functionalization of Carbon Nanotubes. *J. Am. Chem. Soc.* **2002**, *124*, 760–761. (b) Tasis, D.; Tagmatarchis, N.; Bianco, A.; Prato, M. *Chem. Rev.* **2006**, *106*, 1105–1136. (c) Singh, P.; Campidelli, S.; Giordani, S.; Bonifazi, D.; Bianco, A.; Prato, M. Organic Functionalisation and Characterization of Single Walled Carbon Nanotubes. *Chem. Soc. Rev.* **2009**, *38*, 2214–2230.
14. (a) Maggini, M.; Scorrano, G.; Prato, M. The Addition of Azomethine Ylides to C_{60}: Synthesis, Characterization and Functionalized of Fullerene-Pyrrolidines. *J. Am. Chem. Soc.* **1993**, *115*, 9798–9799. (b) Tagmatarchis, N.; Prato, M. The Addition of Azomethine Ylides to [60] Fullerenes Leading to Fulleropyrrolidines. *Synlett* **2003**, *6*, 768–779.
15. (a) Prato, M. [60] Fullerene Chemistry for Material Science Applications. *J. Mater. Chem.* **1997**, *7*, 1097–1109. (b) Tagmatarchis, N.; Prato, M. Functionalization of Carbon Nanotubes *via* 1,3-dipolar Cycloaddition. *J. Mater. Chem.* **2004**, *14*, 437–439.
16. Lin, T.; Zhang, W. D.; Huang, J.; He, C. A DFT Study of the Amination of Fullerenes and Carbon Nanotubes: Reactivity and Curvature. *J. Phys. Chem. B* **2005**, *109*, 13755–13760.
17. Jiang, D.; Sumpter, B. G.; Dai, S. Unique Chemical Reactivity of Graphene Nanoribbon's Zig-Zag Edge. *J. Chem. Phys.* **2007**, *126*, 134701.
18. After the present work was completed, an article describing a similar procedure appeared in the literature: Georgakilas, V.; Bourlinos, A. B.; Zboril, R.; Steroptos, T. A.; Dallas, P.; Stubos, A. K.; Traplis, C. Organic Functionalisation of Graphene. *Chem. Commun.* **2010**, *46*, 1766–1768.
19. (a) Yoshida, A.; Hishiyama, Y.; Inagaki, M. Exfoliated Graphite from Various Intercalation Compounds. *Carbon* **1991**, *29*, 1227–1231. (b) Valles, C.; Drummond, C.; Saadaoui, H.; Furtado, C. A.; Maoshuai, H.; Roubeau, O.; Ortolani, L.; Monthioux, M.; Penicaud, A. Solutions of Negative Charged Graphene Sheets and Ribbons. *J. Am. Chem. Soc.* **2008**, *130*, 15802–15804.
20. (a) Stankovich, S.; Dikin, D. M. G.; Dommett, H. B.; Kohlhaas, K. M.; Zimney, E. J.; Stach, E. A.; Piner, R. D.; Nguyen, S. T.; Ruoff, R. S. Graphene-Based Composite Materials. *Nature* **2006**, *442*, 282–286.
21. Lomeda, J. R.; Doyle, C. D.; Kosynkin, D. V.; Hwang, W. F.; Tour, J. M. Diazonium Functionalization of Surfactant-Wrapped Chemically Converted Graphene Sheets. *J. Am. Chem. Soc.* **2008**, *130*, 16201–16206.
22. Sarin, V. K.; Kent, S. B. H.; Tam, J. P.; Merrifield, R. B. Quantitative Monitoring of Solid Phase Peptide Synthesis by the Ninhydrin Reaction. *Anal. Biochem.* **1981**, *117*, 147–157.
23. (a) Leff, D.; Brandt, V. L.; Heath, J. R. Synthesis and Characterization of Hydrophobic, Organically-Soluble Gold Nanocrystals Functionalized with Primary Amines. *Langmuir* **1996**, *12*, 4723–4730. (b) Kumar, A.; Mandal, S.; Pasricha, R.; Mandale, A. B.; Sastry, M. Investigation into the Interaction between Surface-Bound Alkylamines and Gold Nanoparticles. *Langmuir* **2003**, *19*, 6277–6282. (c) Zhong, Z.; Patskovsky, S.; Bouvrette, P.; Luong, H. T. J.; Gedanken, A. The Surface Chemistry of Au Colloids and Their Interaction with Functional Amino Acids. *J. Phys. Chem. B* **2004**, *108*, 4046–4052.
24. Pérez-Juste, J.; Pastoriza-Santos, I.; Liz-Marzán, L. M.; Mulvaney, P. Gold Nanorods: Synthesis Characterization and Applications. *Coord. Chem. Rev.* **2005**, *249*, 1870–1901.
25. (a) Jain, P. K.; Eustis, S.; El-Sayed, M. A. Plasmon Coupling in Nanorods Assembly: Optical Absorption, Discrete Dipole Approximation Simulation, and Exciton-Coupling Model. *J. Phys. Chem. B* **2006**, *110*, 18243–18253. (b) Pramod, P; Thomas, K. G. Plasmon Coupling in Dimers of Au Nanorods. *Adv. Mater.* **2008**, *20*, 4300–4305. (c) Funston, A. M.; Novo, C.; Davis, T. J.; Mulvaney, P. Plasmon Coupling of Gold Nanorods at Short Distances and in Different Geometries. *Nano Lett.* **2009**, *9*, 1651–1658.
26. Pastoriza-Santos, I.; Gomez, D.; Perez-Juste, J.; Liz-Marzan, L. M.; Mulvaney, P. Optical Properties of Metal Nanoparticles Coated Silica Spheres: A Simple Effective Medium Approach. *Phys. Chem. Chem. Phys.* **2004**, *6*, 5056–5060.
27. Vial, S.; Pastoriza-Santos, I.; Perez-Juste, J.; Liz-Marzan, L. M. Plasmon Coupling in Layer-by-Layer Assembled Gold Nanorods Films. *Langmuir* **2007**, *23*, 4606–4611.
28. Ferrari, A. C.; Meyer, J. C.; Scardaci, V.; Casiraghi, C.; Lazzeri, M.; Mauri, F.; Piscanec, S.; Jiang, D.; Novoselov, K. S.; Roth, S,; Geim, A. K. Raman Spectrum of Graphene and Graphene Layers. *Phys. Rev. Lett.* **2006**, *97*, 187401-1-253113-3.
29. Gupta, A.; Chen, G.; Joshi, P.; Tadigadapa, S.; Eklund, P. C. Raman Scattering From High-Frequency Phonons in Supported *n*-Graphene Layers Films. *Nano Lett.* **2006**, *6*, 2667–2673.
30. Richardson, M. J.; Johnston, J. H. Sorption and Binding of of Nanocrystalline Gold by Merino Wool Fibres. A XPS Study. *J. Colloid Interface Sci.* **2007**, *310*, 425–430.
31. Gomez-Navarro, C.; Weitz, R. T.; Bittner, A. M.; Scolari, M.; Mews, A.; Burghard, M.; Kern, K. Electronic Transport Properties of Individual Chemically Reduced Graphene Oxide Sheets. *Nano Lett.* **2007**, *7*, 3499–3503.
32. Benne, D.; Maccallini, E.; Rudolf, P.; Sooambar, C.; Prato, M. X-ray Photoemission Spectroscopy Study on the Effects of Functionalization in Fulleropyrrolidine and Pyrrolidine Derivatives. *Carbon* **2006**, *44*, 2896–2903.
33. Kumar, A.; Mukherjee, P.; Guha, A.; Adyantaya, S. D.; Mandale, A. B.; Kumar, R.; Sastry, M. Amphoterization of Colloidal Gold Nanoparticles by Capping with Valine and Their Phase Transfer from Water to Toluene by Electrostatic Coordination with Fatty Amine Molecules. *Langmuir* **2000**, *16*, 9775–9783.
34. Correa-Duarte, M. A.; Pérez-Juste, J.; Sánchez-Iglesias, A.; Giersig, M.; Liz-Marzán, L. M. Align Au Nanorods by Using Carbon Nanotubes as Templates. *Angew. Chem., Int. Ed.* **2005**, *44*, 4375–4378.
35. Kordatos, K.; Da Ros, T.; Bosi, S.; Vazquez, E.; Bergamin, M.; Cusan, C.; Pellarini, F.; Tomberli, V.; Pantarotto, D.; Georgakilas, V.; Spalluto, G.; Prato, M. Novel Versatile Fullerene Synthons. *J. Org. Chem.* **2001**, *66*, 4915–4920.